Mechanical characterization and comparison of different NiTi/silicone rubber interfaces

Thierry Rey, Florence Razan, Eric Robin, S. Faure, Jean-Benoît Le Cam, Grégory Chagnon, A. Girard, Denis Favier

Mechanical characterization and comparison of different NiTi/silicone rubber interfaces

T. Rey[(1)], F. Razan[(3)], E. Robin[(2)], S. Faure[(3)], J.-B. Le Cam[(2)], G. Chagnon[(1)], A. Girard[(4)], D. Favier[(1)]

(1) Université de Grenoble, Laboratoire 3SR, domaine universitaire, 38041 Grenoble cedex 9, France.

(2) Université de Rennes 1, L.A.R.M.A.U.R. - CNRS 6274, Campus de Beaulieu, Bât. 10B, 35042 Rennes Cedex, France.

(3) ENS Cachan Bretagne, Campus de Ker Lann, 35170 Bruz, France.

(4) IETR, Campus de Beaulieu, 35042 Rennes Cedex, France.

Abstract

This paper investigates the effects of different surface treatments on the mechanical resistance of interface between wires of NiTi shape memory alloy and silicone rubber. Three different treatments were used; primer, plasma and combination of both. The wires deoxidation effects have also been studied. In order to characterize the interface properties in such composite material, pull-out tests were carried out by means of a home-made device. This test allows us to evaluate the mechanical resistance of the interface in terms of the maximum force reached during the test. First, results show that the debonding force is not higher after the wires deoxidation. This preparation is therefore not necessary. Second, using a primer PM820 and plasma separately leads to a significant improvment of the mechanical resistance. Third, the combination of these treatments (primer followed by plasma) and a longer time of exposure to the plasma alone get the debonding force higher. Consequently, NiTi/silicone rubber interface improved only by means of plasma offers a new way to obtain biocompatible interfaces in such composite material.

Keywords:
NiTi, silicone rubber, interface, adhesion, composite, plasma, primer

1. Introduction

Shape Memory Alloys (SMA) and more specifically Nickel-Titanium (NiTi) are increasingly used in many applications due to their typical behavior, *i.e.* their superelasticity and their shape memory behavior. This type of materials undergoes relatively large deformations of about 10% without exhibiting any plasticity in the pseudoelastic domain [1]. It allows large deformations too in its shape memory form, but a permanent deformation is observed. In the latter case, it can return to its initial shape by heating. The properties of shape memory alloys can be activated either by

*Corresponding author: Jean-Benoît Le Cam: jean-benoit.lecam@univ-rennes1.fr, Université de Rennes 1, L.A.R.M.A.U.R. - CNRS 6274, Campus de Beaulieu, Bât. 10B, 35042 Rennes Cedex, France. Phone number: +33 223 235 741

mechanical or thermal loadings, that explains their large use, especially in the biomedical field and in the aerospace. New categories of innovative materials can be developed by combining the intrinsic properties of these SMA with purposely engineered topologies [2] or with intrinsic properties of other materials such as polymers [3] or elastomers [4]. To realize these unique structures, innovative materials processing techniques are applied such as electrical resistance welding to link NiTi tubes [5], or embedding of NiTi in a polymer matrix [6].

The efficiency of these composites strongly depends on the adhesion between the NiTi and the polymer matrix. Some investigations to improve this adhesion have already been reported in the literature. They highlight that numerous treatments can change the quality of the interface. Neuking *et al.* [7] observed that the adhesion between NiTi wires and a thermoplastic polymer can be improved by a combination of mechanical, physical and chemical surface treatments. Smith *et al.* [8] showed the efficiency of silane coupling agents to improve the interface between NiTi wires and a PMMA matrix. For NiTi/epoxy composites, Jonnalagadda *et al.* [9] showed that the debonding force can be significantly increased by sandblasting the NiTi wires. This treatment is efficient but not suitable for all applications, typically for very little NiTi specimens, due to the sand particles size. In [10], NiTi wires were twisted and next embedded in an epoxy matrix. The geometrical changes and the increase of roughness (by mechanical breaking of the surface oxide film of the wire due to the twisting process) increase the bonding strength. Once again, this treatment seems to be efficient, but it is only possible for the use of wires, and an unrecoverable strain can appear on the wires in the case of a too great number of turns.

Even though numerous studies were carried out on NiTi/polymer interfaces, the interface between NiTi and a silicone rubber has rarely been investigated. Nevertheless, a main result has already been obtained: the interface is improved by acid etching and oxidizing the NiTi wires [11]. This NiTi/silicone rubber association is often used, as example for smart structure applications [12] or for actuators [13, 14]. The interface between silicone rubber and other materials has also been studied. In [15], a primer was used to improve the adhesion between polyurethane and silicone. In [16], an argon-oxygen plasma was used to improve adhesion between collagen and silicone.

This paper aims therefore at investigating the interface NiTi/silicone rubber. The materials and devices are presented in section 2. In section 3, results obtained from different treatments on the NiTi wires are presented. More precisely, the effects of deoxidation of NiTi wires and the differences between interfaces made with adhesion promoter and plasma treatment are discussed related to the maximum force reached during mechanical tests. Finally, concluding remarks close the paper.

2. Materials and methods

2.1. Materials

Wires of commercial pseudoelastic NiTi (with a Ni content of 50.8 at.%) shape memory alloy were used. The diameter of the wires is 0.5 mm. The characteristic temperatures of this material were identified by means of a DSC (Differential Scanning Calorimetry), using a TA Q200 differential scanning calorimeter. It consists in a cooling between 120°C and −90°C followed by a heating between −90°C and 120°C. Cooling and heating rates were set at 10°C per minute. A specimen of 20 mg weight was used. The results of the DSC analysis are presented in Fig. 1. Two peaks are observed. They correspond to the austenite (A) to rhombohedral (R) phase transformation (A to R) during the cooling and the reverse transformation (R to A) during the heating. These peaks are interpreted as the A to R and reverse transformations and not as austenite to martensite (M)

phase (and reverse) transformation because the small difference between the two peaks (T_{R-A}-$T_{A-R} \approx 10°C$) and the low latent heats (about 3 J/g) are representative of the A to R and reverse transformations [17]. The R to M phase transformation (and its reverse) is not visible in the DSC, meaning that the temperature of the R to M transformation is lower than $-90°C$.

A curve of a classical load-unload tensile test of the NiTi at room temperature is presented in Fig. 2. This curve presents a first elastic part, followed by a plateau corresponding to a phase transformation (A to M), and an elastic response of martensite phase. A hysteresis loop is observed, as the level of the plateau is different during load and unload.

The polymer matrix considered here is a filled silicone rubber (Bluestar RTV 3428). The mechanical and thermal properties of this material were previously investigated in [18, 19]. Its crystallization and melting temperatures were identified by a DSC (cooling and heating rates: 2°C per minute) at $-66°C$ and $-41°C$ respectively, and the glass transition temperature is lower than $-90°C$ [19]. The material exhibits a hyperelastic behavior and undergoes high strain levels. Moreover, numerous phenomena take place during its deformation. Results of a tensile test with two load-unload cycles are presented in Fig. 3. A stress softening is observed between first and second loads, corresponding to the Mullins effect [20]. Moreover, a difference between the mechanical response during loads and unloads is observed, it is the mechanical hysteresis. Finally, a little residual elongation is observed after unloading.

A PM820 primer from Bluestar Silicone is used in some cases as an adhesion promoter. It is recommended by Bluestar Silicone to improve the adhesion between a metallic surface and an elastomer.

2.2. Samples preparation

A home-made mold was designed to ensure the NiTi wire to be located in the center of the silicone rubber pancake. Moreover, the mold enables to control the thickness of the silicone specimen, as illustrated in Fig. 4a. The dimensions of the pancake composite are given by the schematic diagram in Fig. 4b. Once the treated wire was put in the mold, the silicone, which was previously blended with its curing agent and degassed to remove air bubbles, was injected by the way of a medical syringe. Then, the mold was put in an oven for 4 hours at 70°C for the silicone curing.

2.3. Surface preparations

The NiTi wires were treated with different techniques: primer, plasma, and combination of both. In order to determine whether oxides at the wire surface affect the interface resistance, a chemical attack is performed to remove the oxides. It consists in immersing the wire in a chemical solution ($1HF+4HNO_5+5H_2O$) during 50 s, and then cleaning it within distilled water. The aim of this preparation is not really considered as one specific treatment such as primer or plasma, but a cleaning of the wire surface.

The first treatment carried out to improve the mechanical resistance of the interface was the application of a thin and uniform coat of the adhesion promoter previously presented. It was applied with a suitable brush. The second treatment corresponds to plasma, with air as working gas. This treatment is performed with a Harrick Plasma Cleaner equipment in clean room and under vacuum set at 10^{-3} mbar. During the treatment, the power was set at 30 W and the exposure time was set either at 600 s or at 1800 s (in the following, it will be precised when the time of plasma is 1800 s). Plasma treatments were already used with NiTi but not in air, for example the modifications of the NiTi surface by air/H_2 plasma and oxygen plasma were studied in [21] and

[22] respectively. The use of this treatment to improve interfaces adhesion was already carried out, as in [23] between steel surfaces and an epoxy matrix, using O_2/Ar microwave plasma treatment.

2.4. Pull-out tests

Pull-out tests were performed to quantify the adhesion between the NiTi wire and the polymer, as classically done in the litterature [7, 8, 10, 11], because adhesion strength increase is linked to the increase of the required force to start the debonding.

These tests were carried out using a Instron 5543 testing machine, which load cell capacity is 1 kN. A second load cell, which capacity is 250 N, was also used.

Fig. 5 shows the experimental device. As the polymer matrix of the studied composite is a soft material, its displacements during the pull-out test can alter the measured adhesion strength. That is why the sample was left in the mold during the test. The mold was mounted in a home-made device, which avoids the translations but allows the mold to rotate. Thus, no flexion is induced in the wire at the beginning of the test. The wire was gripped in a jaw to be pulled out in the vertical direction, at room temperature with a displacement speed of 0.6 mm/s.

2.5. Measurement of the wire deformation

In order to measure wire deformation during the tests, a marks tracking method was used. This method, which is based on image processing technique, allows us to track automatically the position of each marks painted at the wire surface. The position of each mark barycenter is given by:

$$\begin{cases} x_g = \dfrac{\sum_i x_i \left(I_i - I_s\right)}{\sum_i \left(I_i - I_s\right)} \\ y_g = \dfrac{\sum_i y_i \left(I_i - I_s\right)}{\sum_i \left(I_i - I_s\right)} \end{cases} \tag{1}$$

where I_i is the grey level of the pixel, whose coordinates are (x_i, y_i), and I_s is the threshold value, from which the pixels of markers are distinguished [24]. Fig. 6 illustrates the marks tracking method applied.

2.6. Scanning Electron Microscopy

In order to examine the wire surfaces after extracting it, scanning electron microscopy (SEM) was carried out with a JEOL JSM 6301F. An energy dispersive spectrometer of X-rays (EDSX), coupled with a JEOL JSM 6400 microscope, was used to determine the chemical elements on fracture surfaces.

The aim of such analyzes is to compare the effects of different treatments on the interface resistance at the microscopic scale.

3. Results and discussion

The mechanical results, SEM observations and EDSX analysis are presented and discussed in this section.

3.1. Untraited and deoxidized wires

Fig. 7a presents the SEM observation of untreated NiTi wire surface. The surface observation highlights that surface is composed of grains, which differ in shape and in size. Voids, which appear in black color, are observed between grains. EDSX analysis of untreated (Fig. 8a) and deoxidized (Fig. 8b) wire surface confirms the higher amount of oxides in case of untreated wire surface. SEM observations of a deoxidized wire are presented in Fig. 7b. Significant change in the wire surface is observed. Indeed, grains and voids in between are not observed any more, and the surface is composed of cups with different dimensions. The surface is less regular than the previous one, which should promote physical interactions with the rubber matrix.

Fig. 9 presents the results of the pull-out test for an untreated and a deoxidized wire. Debonding occurs for small jaw displacement, with a small force. This debonding force in the case of a deoxidized wire is slightly higher than that of the untreated wire (about 8 N for the first one against about 7 N for the second), but the improvement is not very significant here. The deoxidation of the wire is therefore not necessary to promote the interface properties. After reaching the debonding force, a residual force is measured. It corresponds to the force required to finish the wire extraction. It is due to the friction between the NiTi wire and the silicone rubber matrix.

3.2. Use of an adhesion promoter

The adhesion promoter previously presented is used here to improve interface properties between the NiTi and the silicone matrix. The EDSX analysis of a wire with a primer coat is presented in Fig. 8c. It shows that this adhesion promoter is principally composed of silicon and oxygen, which allows silicone rubber and NiTi to be chemically linked. Indeed, the efficiency of silane (composed too of silicon and oxygen) coupling primers to improve the adhesion in an elastomer-metal interface was already investigated in the literature, as for example in [25].

The results of the pull-out test are presented in Fig. 10 for wires deoxidized or not using the primer, and compared to the results with an untreated wire. The maximum force required to extract the wire of the rubber matrix (55 N) is about eight times higher than previously (7 N), regardless if the wire is deoxidized or not. Moreover, the displacement needed for the debonding is also larger. The curve of the deoxidized and not wires are almost similar, even if the maximum force is a bit higher for an untreated wire using primer. The pull-out curves present some singularities. Firstly, the evolution of the curve is not the same at the beginning of the test (for a displacement between 0 and 0.5 mm) than in the following. The fact that no pre-stress is applied to the test device before the test explains this difference. The device and the specimen have a slight out-of-plane displacement. Secondly, a first peak is observed on the force-displacement curve for a displacement about 2 mm. This phenomenon is often observed in the literature for pull-out tests with NiTi wires. The interpretation of a sliding at the interface is proposed in [11] to explain the first singularity of the curve. The phase changes are raised in [8] to interpret this phenomenon as an elbow and in [26] to justify the numerous peaks in the curve. The transformation possibilities of a pulled out SMA fiber are also put forward in [27], and the effects of the martensitic transformation on a NiTi/polymer composite behavior are investigated in [28]. In the present study, the deformation of the pulled-out wire was determined by the target tracking performed during the test. The results of the measured stress versus the deformation of the wire, until the debonding, are plotted on a strain-stress curve and compared to a NiTi wire subjected to a load-unload uniaxial tensile test in Fig. 11. The strain-stress curve of the pulled-out wire is similar to the uniaxial tensile one, and it can be observed that the strain (0.75 %) and stress (295 MPa) levels reached are clearly not enough

to induce a phase transformation (1.76 % and 475 MPa respectively). The peak on the pull-out curves in Fig. 10 is therefore not explained by a material phase transformation, and seems rather to be a first sliding at the interface of the composite in our case. It is to note that target tracking and study of the wire deformation was done for each test but are not reported in the paper, as the strain and stress never reached the level necessary to start the martensitic transformation.

SEM observations of the extracted wire with primer are shown in Fig. 7c. Even though no silicone rubber was observed on the wire surface, the coat of primer is almost unaltered, excepted a hole where the primer has been extracted. Cracks due to this extraction do not propagate. So the interface between wire and primer is stronger than that between the primer and the silicone rubber matrix as no silicone rubber is remained on the primer coat. Nevertheless, the primer coat is lower in the case of a deoxidized wire as shown in Fig. 7d. A great part of this coat was extracted and stayed in the silicone matrix. The irregularity of the surface of the deoxidized wire leads to a non-uniformity in the primer coat thickness. This leads to crack occurrence in the primer coat, which makes it less efficient.

3.3. Plasma treatment

Fig. 12 presents the results of the pull-out tests using a plasma treatment. Once again, the force required to reach the complete debonding (50 N) is much higher than without treatment (7 N). As for the use of primer, curves exhibit a first peak before increasing again, until reaching the maximum debonding force. As observed previously, results with a deoxidized wire is a little lower than plasma on untreated wire, that is why no more tests are carried out with deoxidized wires.

A wire treated with plasma and extracted from the polymer matrix was observed by SEM (Fig. 7e). A few silicone rubber patches were observed on the wire surface, meaning that some cohesive failures take place in the material before adhesive failure at the interface. The boxed zone magnification in Fig. 7e shows that no difference in the surface morphology is observed between wire with plasma treatment and untreated wire. Moreover, EDSX analysis (Fig. 8d), carried out on a part of the wire surface with silicone rubber, does not allow us to detect any changes in the chemical composition of the pulled wire surface.

3.4. Toward an improvement

The two treatments previously applied have shown efficient results to improve mechanical resistance of the interface. In this section, an additional improvement is researched using these methods. Numerous possibilities exist and it is not possible to cover all of them in the present paper. Here, two methodologies were chosen. The SEM analyzes have shown that using a primer no silicone rubber remains on the primer coat after wire extraction, meaning that the primer-silicone interface was of low resistance. This is why the first method chosen is the application of a plasma treatment on a coat of primer applied on a wire. The second method chosen is a change of the parameters of the plasma treatment, more especially exposure time. Here, the wire is exposed to the plasma during 1800 s against 600 s previously, using the same device. Results of the pull-out tests are presented in Fig. 13. They are quite similar between the two treatments: the level of the first peaks (45 N) and of the maximum forces (about 80 N) are almost the same. The required force and displacement to obtain the complete debonding are very high (more than ten times superior than without treatment), which proves the efficiency of these treatments.

SEM observations of the extracted wire treated with a primer followed by a plasma are shown in Fig. 7f. The primer coat remains at the wire surface, but some silicone rubber patches are observed, which is in good agreement with the improvement of the primer-silicone rubber interface.

The observations carried out on the wire treated with plasma and extracted are not represented here as no difference was observed with the first plasma treatment, *i.e.* a few silicone rubber patches are staying on the wire surface and the microstructure of this one is similar to a untreated wire.

In order to compare and to summarize the results, two diagrams are built. As wire deoxidation does not influence the results, the corresponding results are not represented in these diagrams. In Fig. 14, the maximum forces reached during pull-out tests are plotted. The primer followed by plasma treatment exhibits the higher debonding force (about 80N), leading to a debonding force almost ten times superior to that obtained with an untreated wire. The force reached with a modified plasma treatment is almost the same, whereas the primer and plasma treatment used separately leads to lower force. The untreated wire does not lead to significant improvement of the interface mechanical resistance. Fig. 15, presents the initial curve slopes obtained during the tests (in N/mm). These slopes are calculated before the beginning of the debonding process, *i.e.* before the first peak on each curve. It can be seen here that the increase in the initial slope is less important than for the forces compared to the untreated wire (about two and a half times greater here). The initial curve slopes are almost the same for all the treatments, meaning that all the treatments lead to the same initial mechanical property, but differences appear after the first peak.

4. Conclusion

Different methods to improve the adhesion between NiTi and silicone were tested in this study. First, NiTi wire deoxidation shows no beneficial effects on the mechanical interface resistance. Second, significant improvements of the interface resistance were obtained using a primer and a plasma. The two treatments were found to bring equivalent improvement of the interface. Third, the combination of both primer and plasma (primer then plasma in fact), and a longer exposure time for plasma leads to the best mechanical resistance reinforcement. Even if the primer followed by a plasma presents the better mechanical results, the plasma treatment with an exposure time presents more advantages as it can be applied in various cases contrary to the primer treatment, typically if we consider wire tangle. Finally, this study opens a new route on the elaboration of biocompatible interfaces between NiTi and silicone rubbers, which is currently investigated by the authors.

Acknowledgement

This work is supported by the French National Research Agency Program n2010BLAN90201 ANiM (Architectured NiTi Materials).

References

[1] D. Favier, Y. Liu, L. Orgas, A. Sandel, L. Debove, P. Comte-Gaz, Influence of thermomechanical processing on the superelastic properties of a Ni-rich nitinol shape memory alloy, Mater. Sci. Eng A 429 (2006) 130–136.

[2] G. Machado, H. Louche, D. Do Than, D. Favier, Y. Liu, Experimental characterization and modeling of the mechanical behavior of architectured tube-based NiTi materials, in: The International Conference on Shape Memory and Superelastic Technologies, 2013.

[3] C. J. de Araùjo, L. F. A. Rodrigues, J. F. Coutinho Neto, R. P. B. Reis, Fabrication and static characterization of carbon-fiber-reinforced polymers with embedded NiTi shape memory wire actuators, Smart Mater. Struct. 17 (2008) 065004.

[4] F. Tissot, T. Rey, L. Heller, N. Connesson, G. Chagnon, Y. Payan, D. Favier, P. Sittner, Experiments and modeling of smart silicone elastomer membranes reinforced with shaped NiTi textiles, in: 8th EUROMECH - Solid Mechanics Conference, 2012.

[5] V. Delobelle, P. Delobelle, Y. Liu, D. Favier, H. Louche, Resistance welding of NiTi shape memory alloy tubes, J. Mater. Process. Tech. 213 (2013) 1139–1145.

[6] K. Neuking, A. Abu-Zarifa, S. Youcheu-Kemtchou, G. Eggeler, Polymer/NiTi-composites: Fundamental aspects, processing and properties, Adv. Eng. Mater. 7 (2005) 1014–1023.

[7] K. Neuking, A. Abu-Zarifa, G. Eggeler, Surface engineering of shape memory alloy/polymer-composites: Improvement of the adhesion between polymers and pseudoelastic shape memory alloys, Mater. Sci. Eng., A 481 (2008) 606–611.

[8] N. Smith, G. Antoun, A. Ellis, W. Crone, Improved adhesion between nickel–titanium shape memory alloy and a polymer matrix via silane coupling agents, Compos. Part A-Appl. S. 35 (2004) 1307–1312.

[9] K. Jonnalagadda, G. Kline, N. Sottos, Local displacements and load transfer in shape memory alloy composites, Exp. Mech. 37 (1997) 78–86.

[10] K. Lau, W. Tam, W. Meng, L. Zhou, Morphological study on twisted NiTi wires for smart composite systems, Mater. Lett. 57 (2002) 364–368.

[11] S. Sadrnezhaad, N. Nemati, R. Bagheri, Improved adhesion of NiTi wire to silicone matrix for smart composite medical applications, Mater. Design 30 (9) (2009) 3667–3672.

[12] L. Heller, D. Vokoun, P. Šittner, H. Finckh, 3D flexible NiTi-braided elastomer composites for smart structure applications, Smart Mater. Struct. 21 (2012) 045016.

[13] L. J. Garner, L. N. Wilson, D. C. Lagoudas, O. K. Rediniotis, Development of a shape memory alloy actuated biomimetic vehicle, Smart Mater. Struct. 9 (2000) 673–683.

[14] Chemisky, Modélisation du comportement macroscopique des alliages à memoire de forme - application aux matériaux composites, Ph.D. thesis, Université Paul Verlaine de Metz (2009).

[15] P. P. Chang, N. A. Hansen, R. D. Phoenix, T. R. Schneid, The effects of primers and surface bonding characteristics on the adhesion of polyurethane to two commonly used silicone elastomers, J. Prosthodont. 18 (2009) 23–31.

[16] J. Hauser, J. Zietlow, M. Kőller, S. A. Esenwein, H. Halfmann, P. Awakowicz, H. U. Steinau, Enhanced cell adhesion to silicone implant material through plasma surface modification, J. Mater. Sci.: Mater. Med. 20 (2009) 2541–2548.

[17] D. Favier, Y. Liu, Restoration by rapid overheating of thermally stabilised martensite of NiTi shape memory alloys, J. Alloy. Compd. 297 (2000) 114–121.

[18] G. Machado, G. Chagnon, D. Favier, Induced anisotropy by the Mullins effect in filled silicone rubber, Mech. Mater. 50 (2012) 70–80.

[19] T. Rey, G. Chagnon, J.-B. Le Cam, D. Favier, Influence of the temperature on the mechanical behaviour of filled and unfilled silicone rubbers, Polym. Test. 32 (2013) 492–501.

[20] L. Mullins, Effect of stretching on the properties of rubber, Rubb. Chem. Technol. 21 (1948) 281.

[21] X. Ju, H. Dong, Plasma surface modification of NiTi shape memory alloy, Surf. Coat. Technol. 201 (2006) 1542 – 1547.

[22] L. Tan, W. Crone, Surface characterization of NiTi modified by plasma source ion implantation, Acta Mater. 50 (2002) 4449 – 4460.

[23] J. A. S. Ting, L. M. D. Rosario, M. C. C. Lacdan, H. V. Lee Jr., J. C. De Vero, H. J. Ramos, R. B. Tumlos, Enhanced adhesion of epoxy-bonded steel surfaces using O2/Ar microwave plasma treatment, Int. J. Adhes. Adhes. 40 (2013) 64 – 69.

[24] V. Chean, E. Robin, R. E. Abdi, J.-C. Sangleboeuf, P. Houizot, Use of the mark-tracking method for optical fiber characterization, Opt. Laser Technol. 43 (2011) 1172 – 1178.

[25] B. Golaz, V. Michaud, J.-A. Månson, Adhesion of thermoplastic polyurethane elastomer to galvanized steel, Int. J. Adhes. Adhes. 31 (2011) 805 – 815.
[26] L. Hamming, X. Fan, P. Messersmith, L. Brinson, Mimicking mussel adhesion to improve interfacial properties in composites, Compos. Sci. Technol. 68 (2008) 2042 – 2048.
[27] X. Wang, G. Hu, Stress transfer for a SMA fiber pulled out from an elastic matrix and related bridging effect, Compos. Part A-Appl. S. 36 (2005) 1142 – 1151.
[28] Y. Payandeh, F. Meraghni, E. Patoor, A. Eberhardt, Study of the martensitic transformation in NiTi-epoxy smart composite and its effect on the overall behavior, Mater. Design 39 (2012) 104 – 110.

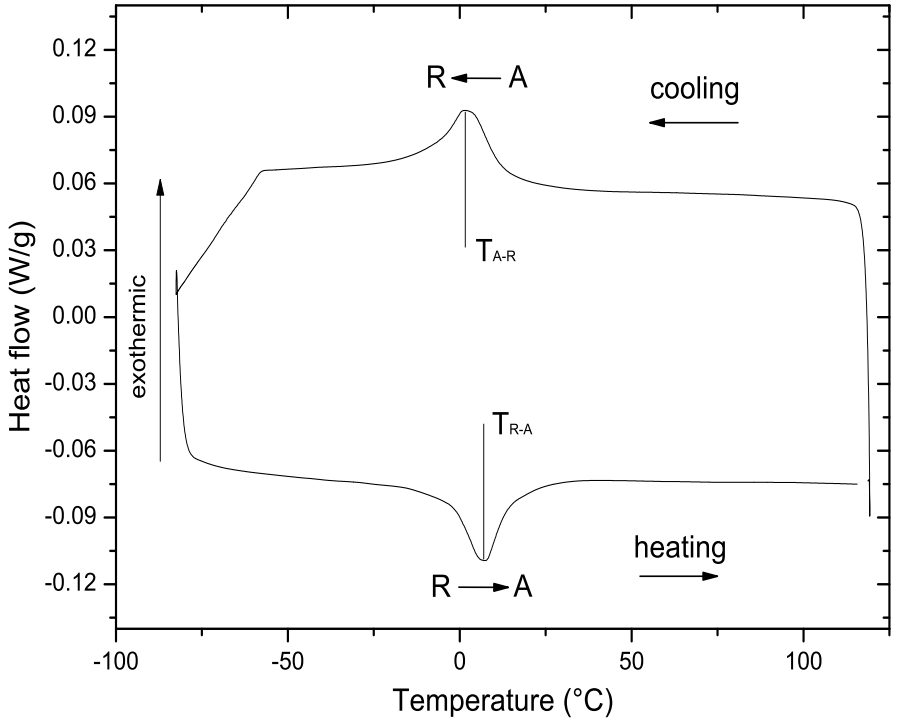

Fig. 1: DSC analysis of the NiTi wire.

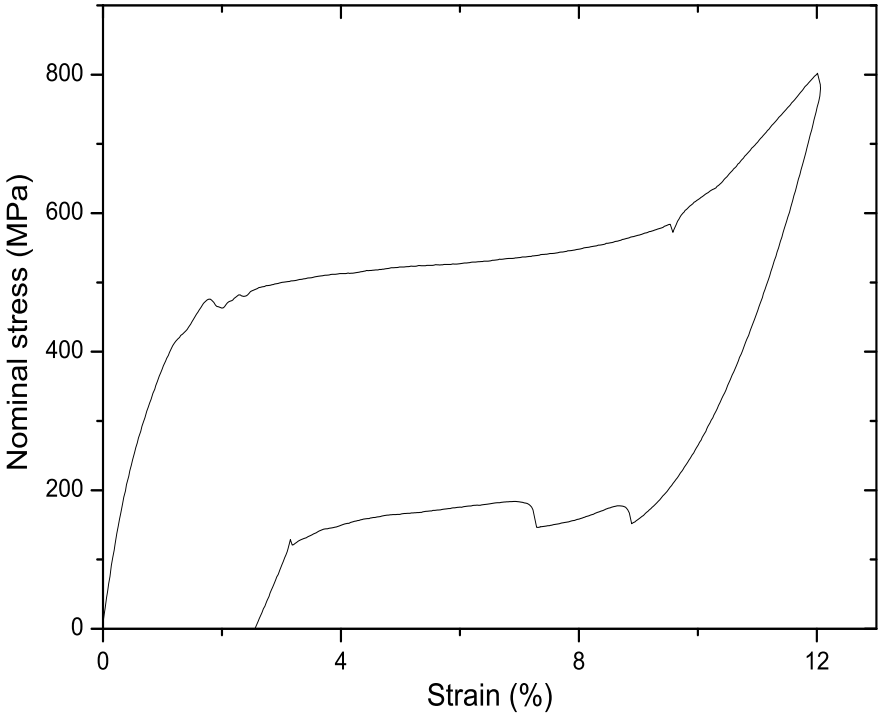

Fig. 2: Load-unload tensile test on a NiTi wire at room temperature.

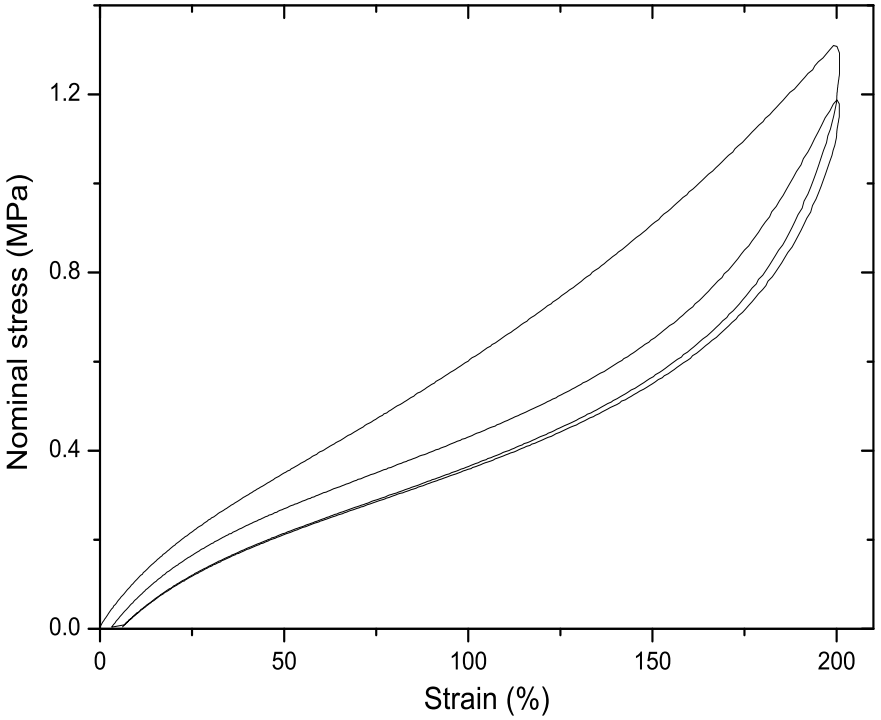

Fig. 3: Load-unload tensile test (two cycles) on a RTV 3428 silicone rubber at room temperature.

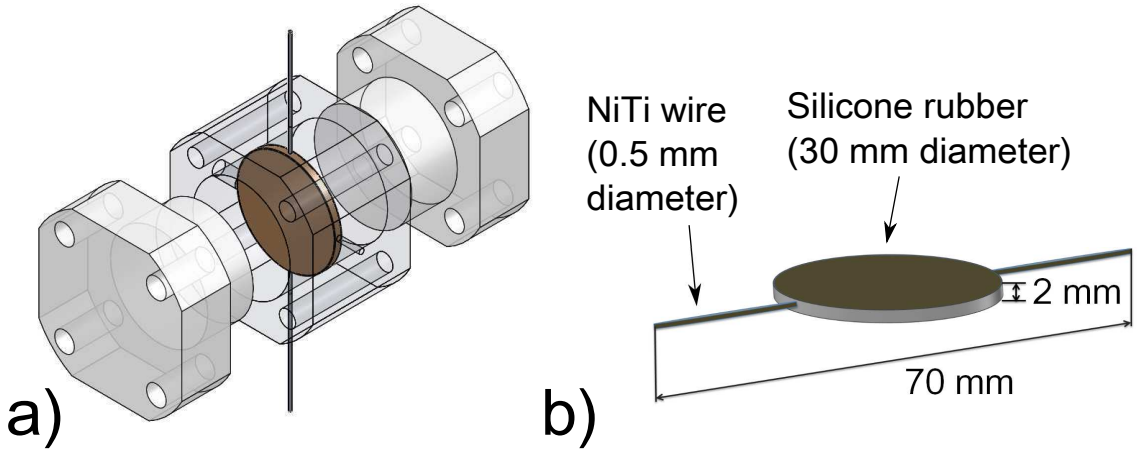

Fig. 4: Elaboration of the NiTi-silicone composite. a) Home-made mold for elaboration and b) scheme of the NiTi-silicone specimen with dimensions.

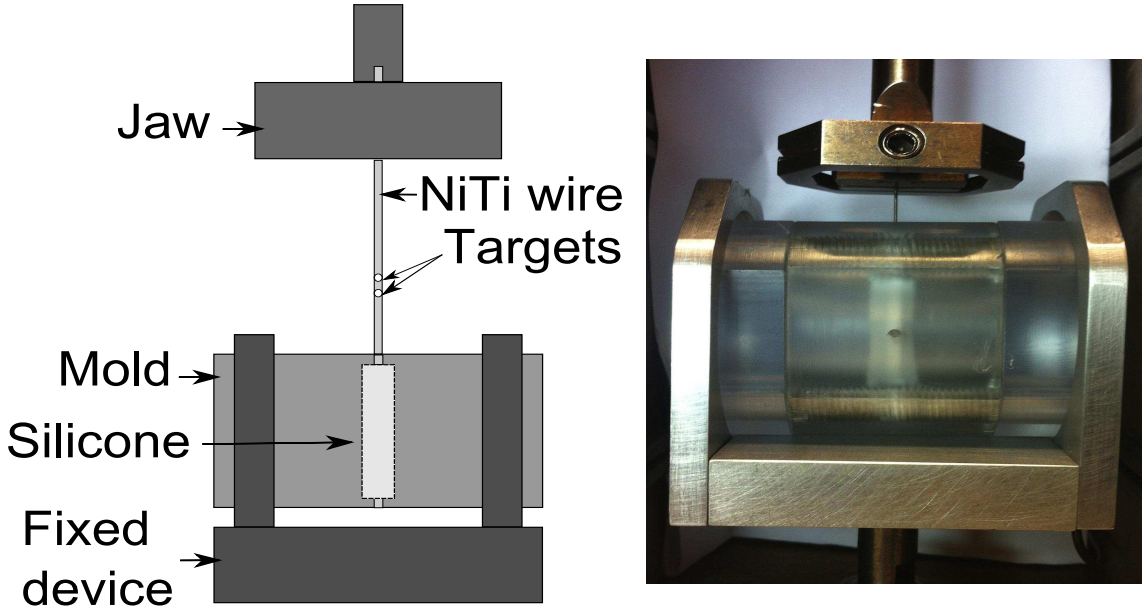

Fig. 5: Pull out device.

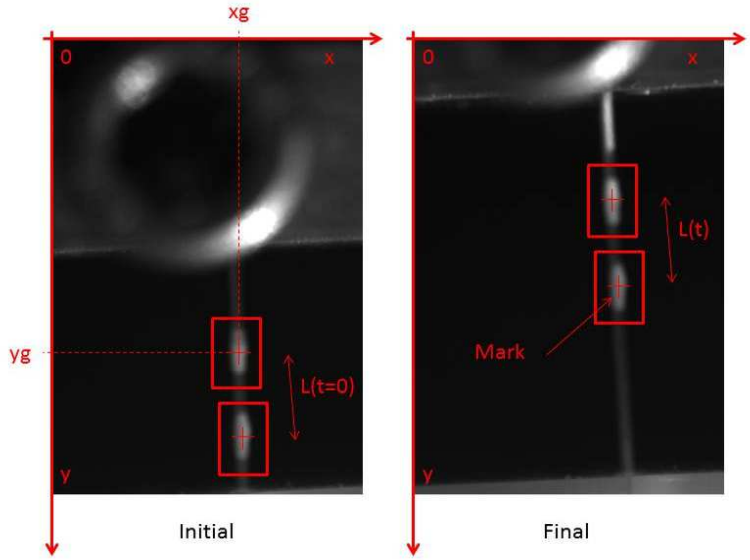

Fig. 6: Pictures illustrating the marks tracking method.

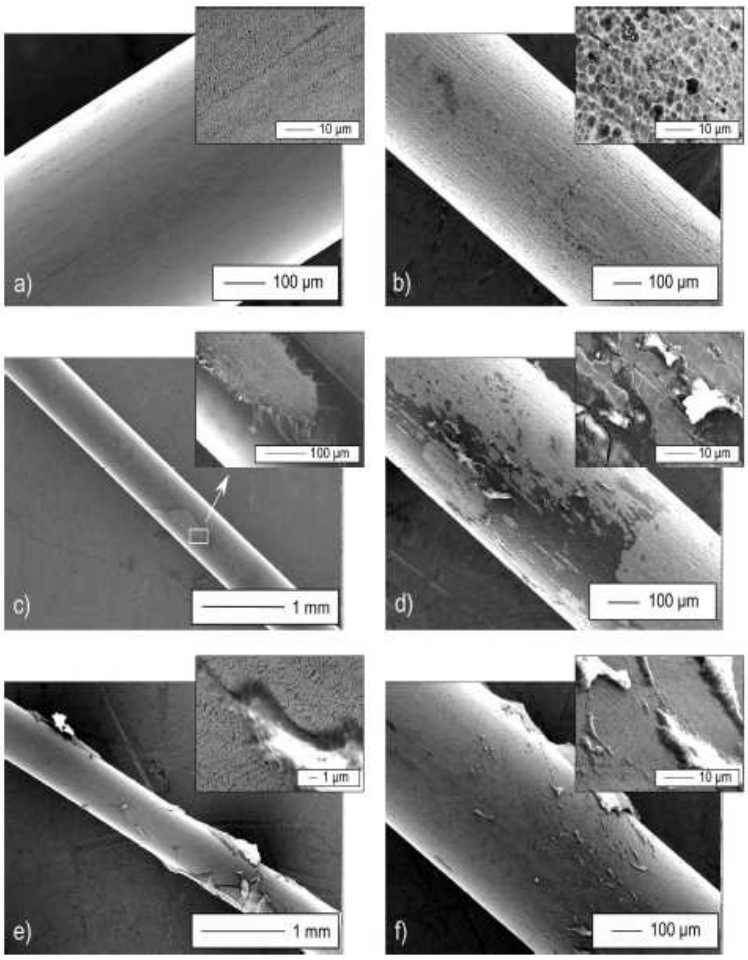

Fig. 7: Observations of the pulled out wires a) without any treatment, b) deoxidized, c) with a primer, d) deoxidized with a primer, e) treated with a plasma and f) with a primer and a plasma treatment.

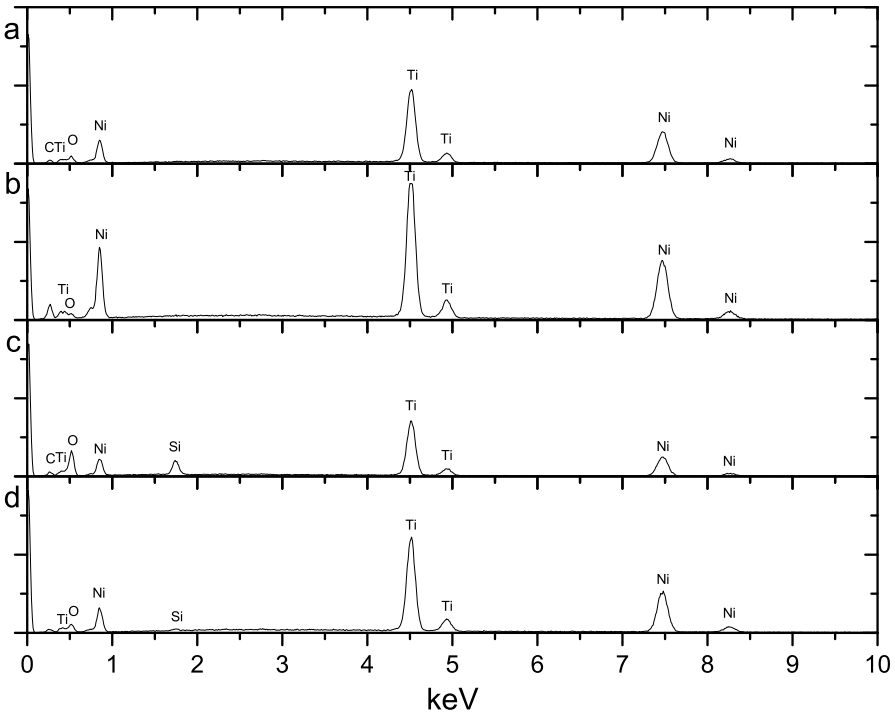

Fig. 8: EDSX analisys of a wire a) without any treatment, b) deoxidized, c) with a primer and d) treated with a plasma.

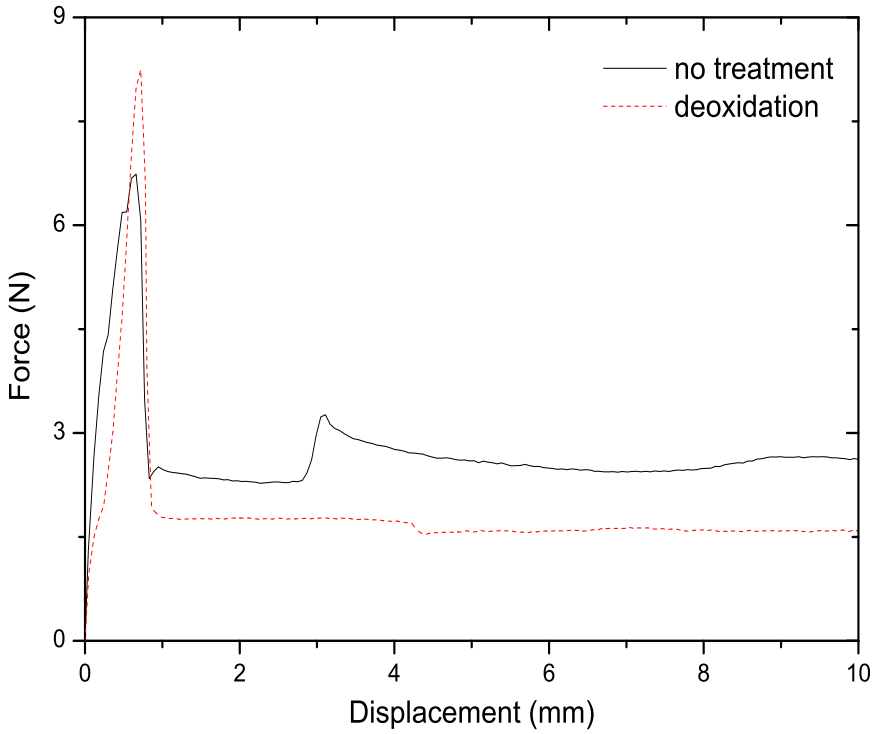

Fig. 9: Results of a pull out test with an untreated and a deoxidized NiTi wire.

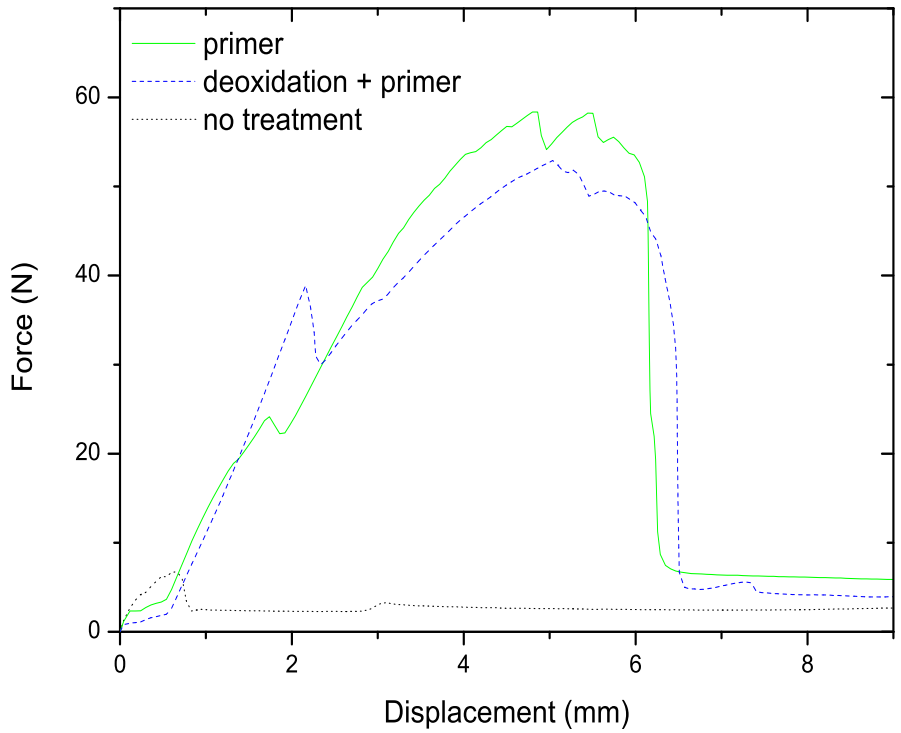

Fig. 10: Effect of the adhesion promoter on the interface NiTi/silicone rubber.

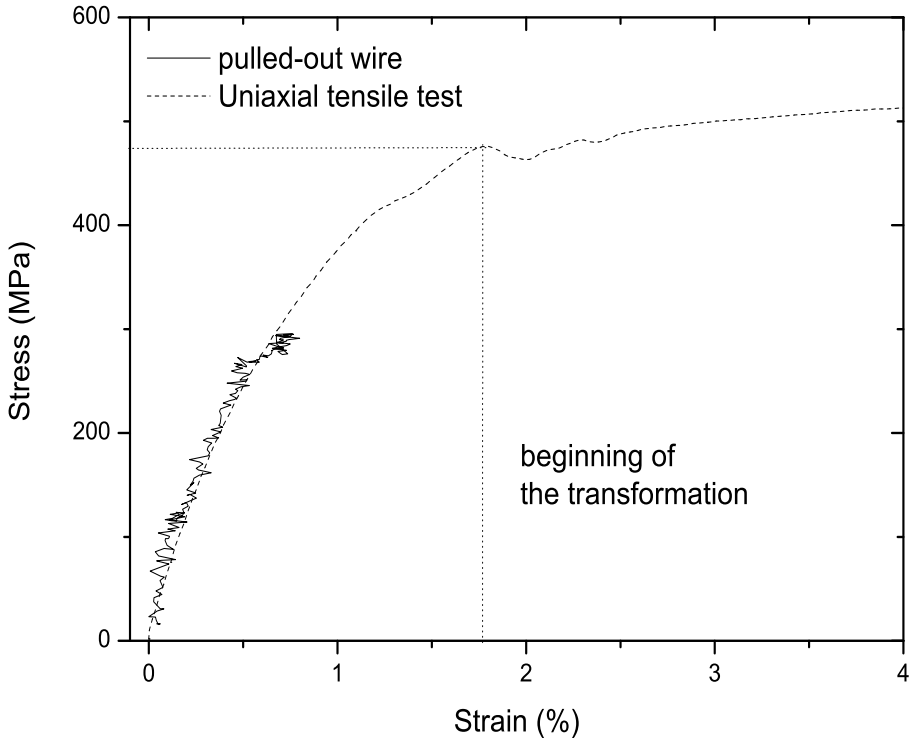

Fig. 11: Deformation of the NiTi wire during the pull out test with a primer treatment, compared to a load-unload cycle of a NiTi wire.

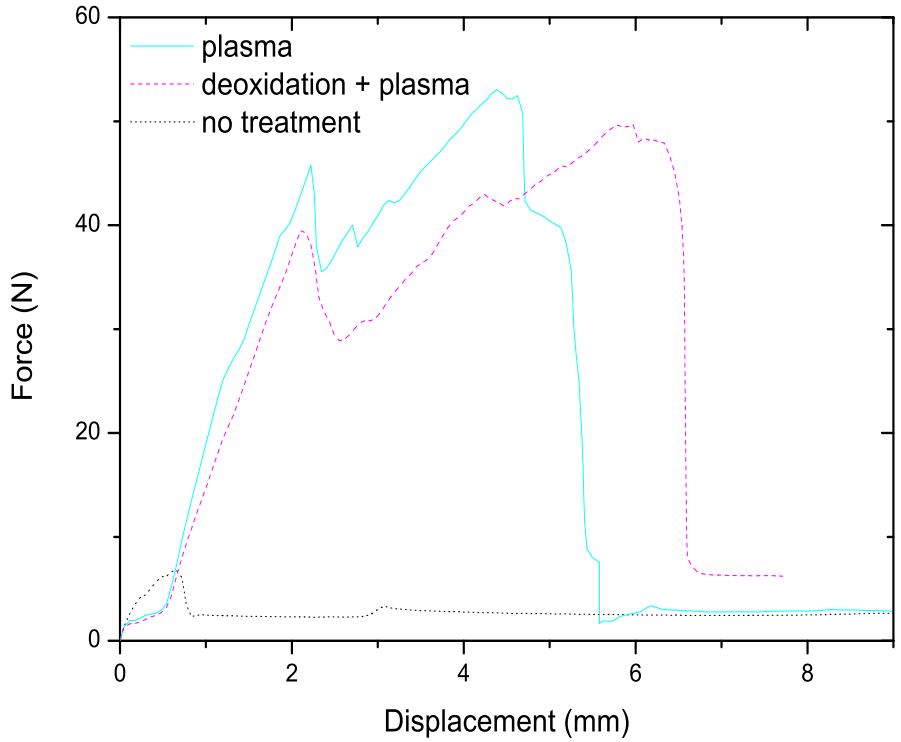

Fig. 12: Plasma treatment effect on the NiTi/silicone rubber interface.

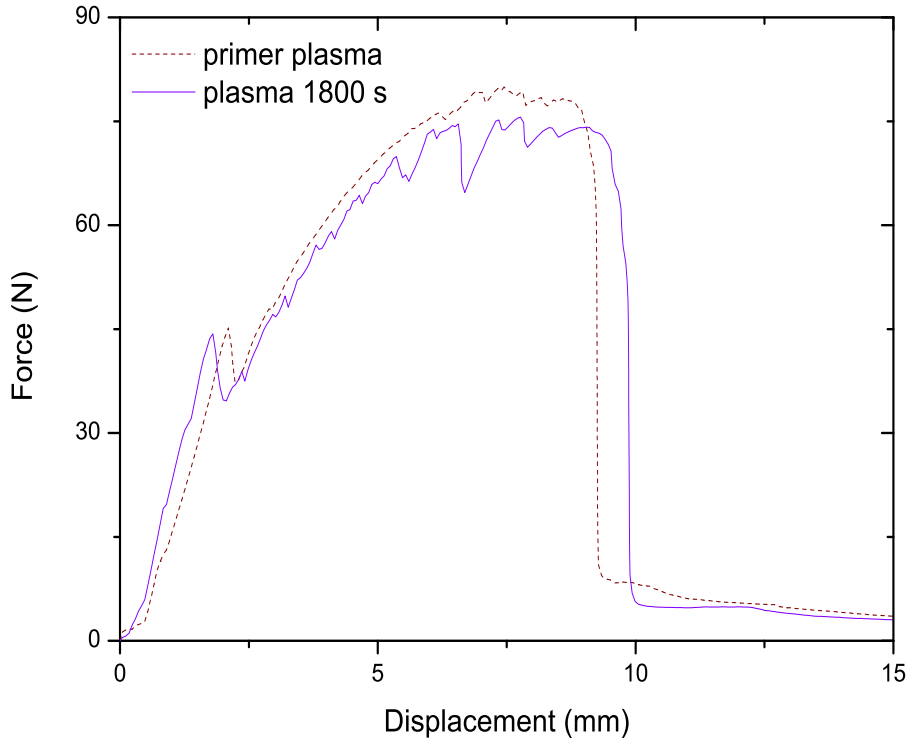

Fig. 13: Effect of a longer time plsma and of primer + plasma on the interface NiTi/silicone rubber.

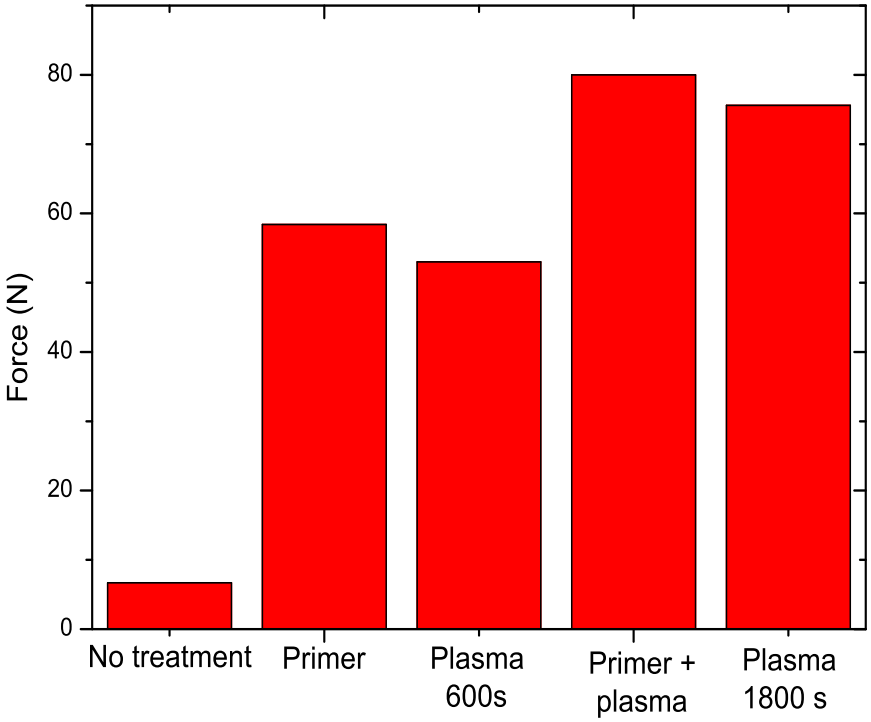

Fig. 14: Maximum force values obtained during a pull out test.

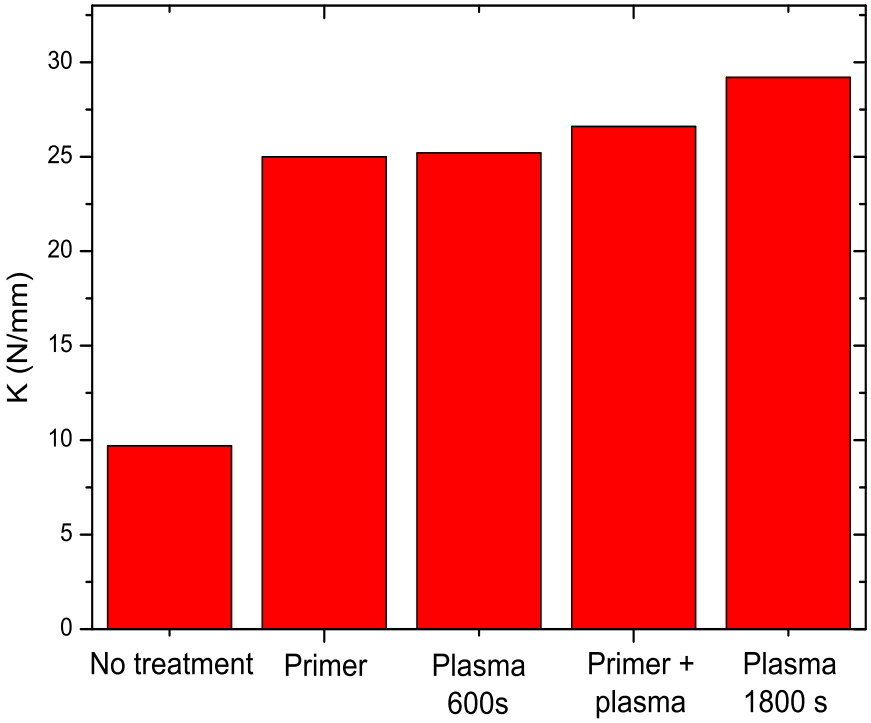

Fig. 15: Initial slopes obtained during a pull out test.